

## CORRECTION

# Paradox of the drinking-straw model of the butterfly proboscis

**Chen-Chih Tsai, Daria Monaenkova, Charles Beard, Peter Adler and Konstantin Kornev**

There was an error published in *J. Exp. Biol.* **217**, 2130-2138. Eqns A12 and A13 in the Appendix were cropped. The online pdf and full-text versions (but not the print version) of the article have been corrected. The correct versions of the equations also appear below.

$$P_p = \frac{1}{\left( \frac{ab}{a+b} - \frac{r^4}{L_p - L} \right)} \left[ \frac{r^4 P_c}{L_p - L} + \frac{\rho g r^4}{L_p - L} (L_p - L) - \frac{\rho g ab L_p}{a+b} \right]. \quad (\text{A12})$$

$$\frac{dL}{dt} = \frac{r^2}{8\eta} \frac{(P_c - \rho g L)}{L - L_p + \frac{r^4(a+b)}{ab}}. \quad (\text{A13})$$

We apologise to the authors and readers for this error.

## RESEARCH ARTICLE

# Paradox of the drinking-straw model of the butterfly proboscis

Chen-Chih Tsai<sup>1</sup>, Daria Monaenkova<sup>1,2</sup>, Charles E. Beard<sup>3</sup>, Peter H. Adler<sup>3</sup> and Konstantin G. Kornev<sup>1,\*</sup>

## ABSTRACT

Fluid-feeding Lepidoptera use an elongated proboscis, conventionally modeled as a drinking straw, to feed from pools and films of liquid. Using the monarch butterfly, *Danaus plexippus* (Linnaeus), we show that the inherent structural features of the lepidopteran proboscis contradict the basic assumptions of the drinking-straw model. By experimentally characterizing permeability and flow in the proboscis, we show that tapering of the food canal in the drinking region increases resistance, significantly hindering the flow of fluid. The calculated pressure differential required for a suction pump to support flow along the entire proboscis is greater than 1 atm (~101 kPa) when the butterfly feeds from a pool of liquid. We suggest that behavioral strategies employed by butterflies and moths can resolve this paradoxical pressure anomaly. Butterflies can alter the taper, the interlegular spacing and the terminal opening of the food canal, thereby controlling fluid entry and flow, by splaying the galeal tips apart, sliding the galeae along one another, pulsing hemolymph into each galeal lumen, and pressing the proboscis against a substrate. Thus, although physical construction of the proboscis limits its mechanical capabilities, its functionality can be modified and enhanced by behavioral strategies.

**KEY WORDS:** Butterfly feeding, Hagen–Poiseuille flow, Lepidoptera, Suction pressure, Wicking phenomena

## INTRODUCTION

Butterflies and moths (Lepidoptera) use their slender proboscises to sip nectar, plant sap, animal tears, blood and other fluids, which are generally complex in composition (Krenn, 2010). The proboscis simultaneously is a multifunctional material and a fluidic device composed of two flexible strands, the maxillary galeae, with C-shaped medial faces joined by cuticular projections, the legulae (Monaenkova et al., 2012) (Fig. 1). The materials organization of the proboscis is unique, enabling it to perform multiple tasks, such as fluid acquisition, environmental sensing, coiling and uncoiling, and self-cleaning (Eastham and Eassa, 1955; Kingsolver and Daniel, 1995; Krenn, 2010).

The size of the dorsal legulae and their spacing significantly increase in the distal 5–20% of the proboscis (Krenn, 2010; Monaenkova et al., 2012). The distal region of the proboscis, which is called the ‘drinking region’, is hydrophilic, while the remaining portion has hydrophobic properties (Lehnert et al., 2013). The drinking region plays a critical role in fluid acquisition, especially for Lepidoptera that feed from porous materials such as rotten fruit. Submicrometer pores (interlegular spaces) in the

proboscis, which is initially air filled, provide strong capillary action favoring the uptake of fluid droplets and films, and facilitating fluid withdrawal from substrate pores (Tsai et al., 2011; Monaenkova et al., 2012). The proboscises of Lepidoptera that feed on porous materials, such as rotten fruit, typically have a brush-like lateral series of chemosensilla that aid fluid uptake (Knopp and Krenn, 2003; Monaenkova et al., 2012; Lehnert et al., 2013). Extant members of ancient lepidopteran lineages also have brushy proboscises (Krenn and Kristensen, 2000), suggesting that capillarity had an early selective advantage, perhaps in exploiting limited moisture and sugary exudates (Kristensen, 1984; Grimaldi and Engel, 2005). To acquire fluid from porous materials and liquid films, butterflies rely on capillary instability in the food canal to partition the fluid into bubble trains and reduce the effective viscosity, relative to a continuous liquid column; the bubble train then facilitates the ability of the cibarial pump to draw fluid into the gut (Monaenkova et al., 2012). Lepidoptera, thus, use the dual action of capillarity and cibarial pumping to acquire fluids from porous materials and films. Evolutionary diversification of siphonate Lepidoptera, including those with comparatively smooth proboscises capable of reaching pools of nectar in floral tubes, was associated with the radiation of flowering plants (Barth, 1991; Grimaldi and Engel, 2005).

The mechanism by which Lepidoptera acquire fluid from a pool has been debated (Kingsolver and Daniel, 1995; Borrell, 2006; Borrell and Krenn, 2006). The drinking-straw model, based on the Hagen–Poiseuille equation (Vogel, 2003), was proposed to explain a relationship between the observed flow rate and the pressure differential required from the cibarial suction pump. This model assumes that the food canal is a straight tube, circular in cross-section (Kingsolver and Daniel, 1979; Kingsolver, 1985; Kingsolver and Daniel, 1995). The drinking-straw model is useful for crude estimates of the effects of food canal diameter and fluid viscosity on the feeding efficiency and energetic requirements (Kingsolver, 1985; Kingsolver and Daniel, 1995). The model faces problems, however, when attempting to interpret experimental observations of the uptake of thick fluids (Lehane, 2005). As revealed by X-ray tomography (Monaenkova et al., 2012), the food canal tapers apically to a microscopic slit-like opening. The complex geometry of the food canal draws into question whether the Hagen–Poiseuille model (Kingsolver and Daniel, 1995) of flow through a cylindrical tube can be applied directly to the butterfly proboscis. The distal taper of the food canal (Krenn and Muhlberger, 2002; Monaenkova et al., 2012) presents a structural problem for the drinking-straw model.

To test the hypothesis that the proboscis can function as a Hagen–Poiseuille straw, we examined permeability and flow in the drinking region of the monarch butterfly, *Danaus plexippus* (Linnaeus).

## Proboscis permeability

The ability of a conduit or porous material to transport fluid at the fixed pressure gradient is characterized by the materials parameter called ‘permeability’ (Scheidegger, 1974; Dullien, 1991), denoted

<sup>1</sup>Department of Materials Science and Engineering, Clemson University, Clemson, SC 29634, USA. <sup>2</sup>School of Physics, Georgia Institute of Technology, Atlanta, GA 30332, USA. <sup>3</sup>School of Agricultural, Forest and Environmental Sciences, Clemson University, Clemson, SC 29634, USA.

\*Author for correspondence (kkornev@clemson.edu)

Received 5 October 2013; Accepted 4 March 2014

**List of symbols and abbreviations**

$a$	$3 \tan \phi R_0^3 R_p^3 / (R_p^3 - R_0^3)$
$b$	$R_p^4 / (L_p - H)$
$c$	$[P_p - P_H + \rho g(L_p - H)] / (L_p - H)$
$d$	$P_p + \rho g L_p - L_p [P_p - P_H + \rho g(L_p - H)] / (L_p - H)$
$A$	cross-sectional area of food canal
DCA	dynamic contact angle
$F$	wetting force
$g$	gravitational acceleration
$H$	length of drinking region
$h_d$	droplet height
$k$	permeability
$k_H$	permeability of the drinking region of the proboscis
$k_p$	permeability of the proboscis
$L$	meniscus position
$L^*$	dimensionless meniscus position
$L_p$	length of proboscis used in experiments
$p$	perimeter
$P$	pressure
$P_c$	capillary pressure
$P_H$	pressure differential at the boundary of the drinking region
$P_p$	pressure differential in the cibarial pump in a tapered food canal
$P_t$	pressure differential in the cibarial pump in a drinking-straw model
$\dot{Q}$	flow rate (liquid discharge per unit time)
$\dot{Q}_c$	flow rate through the capillary tube
$\dot{Q}_H$	flow rate through the drinking region of the food canal
$\dot{Q}_p$	flow rate through the non-drinking region of the food canal
$r$	radius of the capillary tube
$R$	radius of the food canal
$R_0$	radius of the food canal opening
$r_d$	droplet radius
RH	relative humidity
$R_p$	radius of the straight section of the food canal
$t$	time
$t^*$	dimensionless time
$t_0$	characteristic time
$V$	volume
$V_d$	droplet volume
$x$	coordinate
$y$	coordinate
$Z_c$	Jurin height
ZDOI	zero depth of immersion
$\beta$	dimensionless parameter
$\eta$	liquid viscosity
$\theta$	contact angle
$\rho$	liquid density
$\sigma$	surface tension
$\phi$	taper angle
$\Phi$	flow potential

here as  $k$ . Permeability enters the problem via Darcy's law (Scheidegger, 1974; Dullien, 1991), which states that the flow discharge  $\dot{Q}$  through the food canal of cross-sectional area  $A$  and length  $L$  is written as:

$$\dot{Q} = (kA / \eta) (\Delta P / L), \quad (1)$$

where  $\eta$  is the liquid viscosity and  $\Delta P$  is the pressure differential. In particular, if the proboscis is modeled as a cylindrical tube of radius  $r$ , the permeability  $k$  is derived from the Hagen–Poiseuille law as  $k = r^2/8$  (Vogel, 2003). For a more complex geometry, the material parameter  $k$  can be obtained by directly measuring the total flow rate  $\dot{Q}$  and pressure gradient and by knowing the cross-sectional area of the food canal and viscosity of the liquid.

Permeability is a convenient metric for characterizing transport properties of the butterfly proboscis and interlegular pore structure (Monaenkova et al., 2012). Permeability of the interlegular pores in

the non-drinking region can be determined by placing a droplet of water on the dorsal legulae and evaluating its uptake kinetics (Monaenkova et al., 2012). The distances between adjacent legulae of a monarch butterfly were estimated as  $96 \pm 27$  and  $162 \pm 18$  nm at 5 and 10 mm distal to the head, respectively (Monaenkova et al., 2012). This droplet method, however, is not reliable for determining the permeability of the drinking region; the spreading and intake rates of a droplet in the drinking region are comparable.

We therefore developed a new method to evaluate proboscis permeability in the drinking region. A proboscis was inserted into a glass capillary tube and immersed in deionized water (Fig. 2). The food canal of the proboscis was initially filled with air. As a result of capillary forces, water spontaneously invaded the proboscis pores (interlegular spaces) and food canal, moving farther into the capillary tube. When the proboscis was filled with water and a meniscus appeared in the capillary tube, the flow rate was measured directly with a Cahn DCA-322 Dynamic Contact Angle Analyzer. By monitoring incremental changes in the weight of a hanging capillary tube, we were able to evaluate flow rates. The flow rates through the capillary tube and the proboscis were the same, allowing us to specify the flow through the proboscis.

According to Darcy's law, Eqn 1, the pressure differential at point  $y = L_p$  (Fig. 2A), where the proboscis meets the bore, needs to be determined to obtain the permeability of the proboscis. This pressure,  $P_p$ , could not be measured. However, we could estimate the pressure at the meniscus moving in the capillary tube, knowing the contact angle  $\theta$  determined from Jurin's experiments (Jurin, 1917–1919), as previously discussed for this geometry (Tsai and Kornev, 2013), surface tension  $\sigma$  of the liquid and radius  $r$  of the capillary tube. The driving capillary pressure:

$$P_c = 2\sigma \cos \theta / r, \quad (2)$$

thus was obtained independently (Tsai and Kornev, 2013). Once the driving capillary pressure was known, the problem of determining proboscis permeability was reduced to the problem of liquid flow through a composite conduit consisting of two tubes connected in a sequence (Tsai and Kornev, 2013).

When a conduit has a fixed length and the pressure differential is applied to the ends of this conduit, the flow description is reduced to the Cohn–Rashevsky method of design of some parts of the cardiovascular system (Cohn, 1954; Cohn, 1955; Rashevsky, 1960). In the case of a moving meniscus, the length of the liquid column changes with time and the Cohn–Rashevsky model needs to be changed. A more realistic model of a tapered food canal was used and compared with the straight cylinder model. In each tube of the complex conduit, the flow was assumed to follow the Hagen–Poiseuille law, and the conservation of mass and the pressure continuity were used as the boundary conditions at the point where the proboscis met the capillary tube. With this model, the permeability of the capillary tube could be separated from the permeability of the proboscis.

### Interpretation of wicking experiments

The proboscis-in-a-tube system was modeled as a complex conduit consisting of three distinct parts (Fig. 3): (i) the drinking region of length  $H$  where the food canal tapered at angle  $\phi$  and the legular structure changed significantly (Lehnert et al., 2013); (ii) the non-drinking region, an almost straight section of the food canal, modeled as a straight, circular cylinder of inner radius  $R_p$  and length  $L_p - H$ ; and (iii) the capillary tube of inner radius  $r$ . The galeae at the proboscis tip sometimes opened during feeding; hence, we modeled the drinking region as a cylindrical truncated cone with an unknown

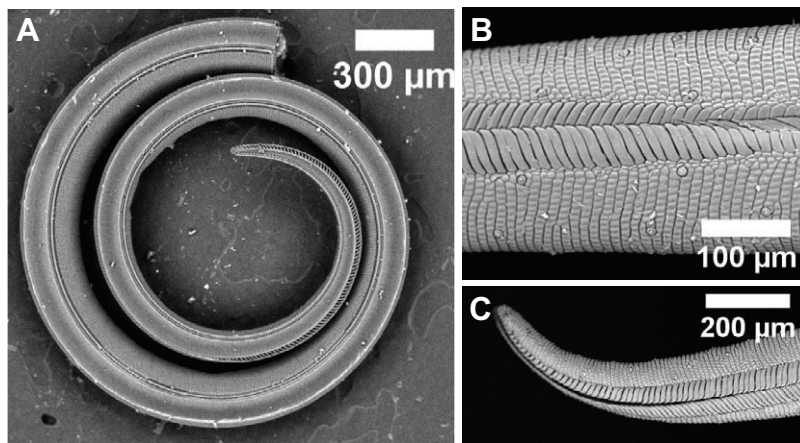


**Fig. 1. Scanning electron micrographs of the monarch butterfly proboscis.** (A) Single galea of the monarch proboscis, with the open food canal facing upward; the taper of the food canal is noticeable only in the drinking region. (B) Dorsal legulae with slit-like pores (interlegular spaces) enabling liquid to enter the food canal. (C) Proboscis tip showing a slit between opposing galeae; the spacing of the gap can change during feeding.

radius at the opening,  $R_0$ . This radius was determined by fitting the experimental data with a developed model. With the proboscis-in-a-tube model as a series of three conduits – a Cohn–Rashevsky-type model of liquid flow through a conduit chain – we applied the basic conservation laws of fluid mechanics to derive the following equation describing the change of length of the liquid column,  $L(t)$  (see Appendix):

$$\frac{dL}{dt} = \frac{r^2}{8\eta} \frac{(P_c - \rho g L)}{L - L_p + \frac{r^4(a+b)}{ab}}, \quad (3)$$

where  $a=3\tan\phi R_0^3 R_p^3/(R_p^3 - R_0^3)$  and  $b=R_p^4/(L_p - H)$ .

#### Engineering parameters of the butterfly proboscis

The derived equation depends on structural parameters of the proboscis and physico-chemical parameters of the liquid. The dynamics of meniscus propagation, however, depend only on a single dimensionless complex. It is convenient to introduce the Jurin height,  $Z_c = 2\sigma \cos\theta/(\rho g r)$ , where  $\rho$  is the liquid density and  $g$  is acceleration due to gravity (Jurin, 1917–1919; Lehnert et al., 2013; Tsai and Kornev, 2013); this is the maximum height that the

meniscus can reach in a given capillary tube. Measuring the time in units as:

$$t_0 = \frac{8\eta Z_c}{\rho g r^2} = \frac{16\eta \sigma \cos\theta}{p^2 g^2 r^3}, \quad (4)$$

which is the time required for a liquid meniscus to reach the Jurin length, we can rewrite Eqn 3 in dimensionless variables  $L^* = L/Z_c$ ,  $t^* = t/t_0$  as:

$$\frac{dL^*}{dt^*} = \frac{1 - L^*}{L^* + \beta}, \quad (5)$$

where:

$$\beta = \frac{r^4(a+b)}{abZ_c} - \frac{L_p}{Z_c}. \quad (6)$$

Eqn 5 is the Lucas–Washburn equation describing capillary rise in tubes (Lucas, 1918; Washburn, 1921), which has the solution:

$$-L^* - (1 + \beta) \ln(1 - L^*) = t^*. \quad (7)$$

In our experiments, the proboscis length was  $\sim 5$  mm, which is smaller than the Jurin height,  $\sim 29$  mm ( $L_p \ll Z_c$ ). Hence, the effect

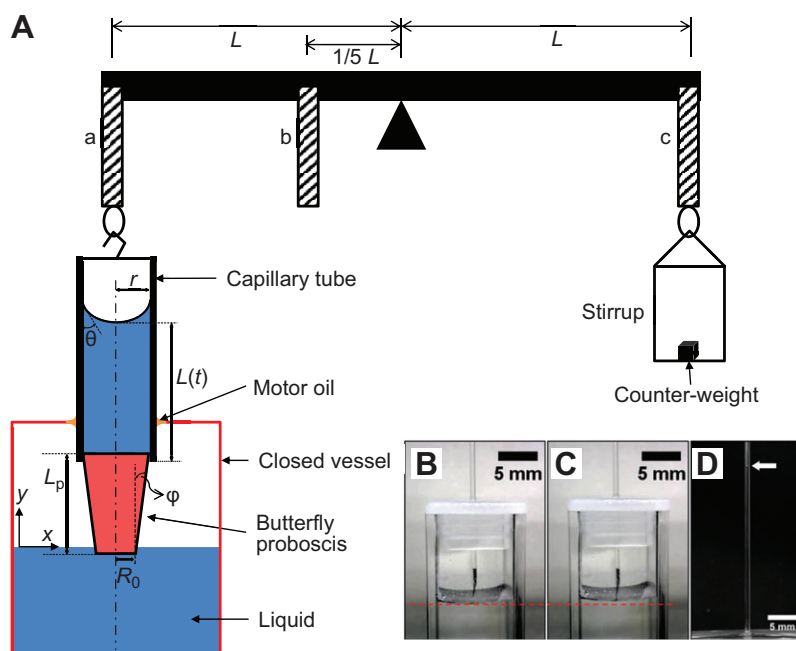


**Fig. 2. Analysis of proboscis permeability.** (A) Schematic diagram of the experiment showing operation of the Cahn DCA-322. A capillary tube with an inserted proboscis is connected to the balance arm by a hook. An oil droplet closes the rectangular vessel, preventing water evaporation and allowing the tube to move freely through the hole. Water moves from the reservoir to the tube by capillary action. The weight of the wicking water column is measured by the balance arm as the meniscus moves up the bore of the capillary tube.  $L$ , meniscus position;  $r$ , radius of the capillary tube;  $\theta$ , contact angle;  $L(t)$ , change in the length of the liquid column;  $L_p$ , length of the proboscis;  $R_0$ , radius of opening;  $\phi$ , taper angle;  $xy$ , the plane of proboscis placement;  $a$ – $c$ , loops (see Materials and methods). (B) Closed vessel after 1 h of saturation with water vapor. The proboscis is suspended above the water. (C) The same vessel at the moment when the proboscis touches the water. (D) Example of measurement of Jurin height ( $Z_c$ ); arrow indicates the meniscus.

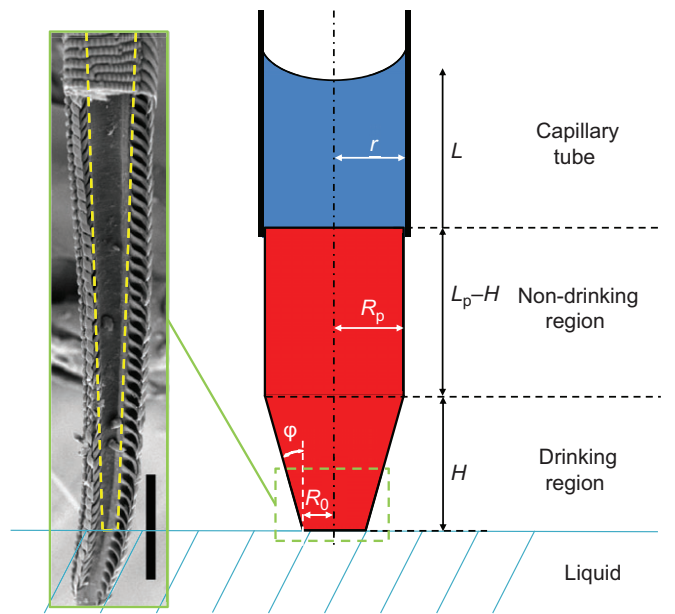


**Fig. 3. Proboscis-in-a-tube model.** Left: proboscis tip with one galea removed to expose the food canal of a monarch butterfly; scale bar, 1 mm. Right: schematic diagram of the food canal model.  $L_p$  is the proboscis length used in wicking experiments,  $H$  is the length of the drinking region,  $R_p$  is the radius of the straight section of the food canal,  $R_0$  is the radius of the opening and  $\phi$  is the taper angle.

of gravity, the second term on the right side of Eqn 6, can be neglected, and Eqn 6 is simplified as:

$$\beta = \frac{r^4(a+b)}{abZ_c} \tag{8}$$

Thus, using the introduced variables, we can interpret the experimental data by measuring the Jurin height  $Z_c$ , calculating the characteristic time  $t_0$ , and then fitting the experimental curve  $L^*(t^*)$  by adjusting parameter  $\beta$ . After determination of this parameter, the length of the drinking region was calculated as  $ab\beta Z_c - r^4(a+b) = 0$ , or:

$$H = \frac{3R_0^3R_p^4Z_c\beta - 3R_0^3R_p^4L_p}{R_p r^4(R_p^2 + R_p R_0 + R_0^2) - 3R_0^3r^4} \tag{9}$$

Taking into account the relationship:

$$R_p = R_0 + H \tan(\phi), \tag{10}$$

the problem of determination of the unknown  $H$  and  $R_0$  is reduced to solution of Eqns 9 and 10.

RESULTS

As an illustration of our experimental protocol, we show the experimental  $L^*$  versus  $t^*$  curve for a single monarch proboscis (Fig. 4). The solid black line was plotted by adjusting the  $\beta$ -parameter to provide the best fit of the model to the experimental data. To determine other physical parameters of the model, we measured Jurin height  $Z_c=29$  mm and parameter  $\phi\approx0.95$  deg from representative scanning electron micrographs, and parameters  $L_p=4.9$  mm and  $R_p=30$   $\mu$ m from optical images. These values were substituted into Eqns 9 and 10 to determine  $R_0=3.4$   $\mu$ m and  $H=1.61$  mm.

Using this protocol, we analyzed the results of the wicking experiments on different proboscises and obtained their average characteristics (Table 1). Parameters  $\phi\approx0.95$  deg,  $L_p=4.9$  mm and  $R_p=30$   $\mu$ m were kept unchanged. The dimensionless parameter  $\beta$ , which depends on the geometrical structure of the butterfly

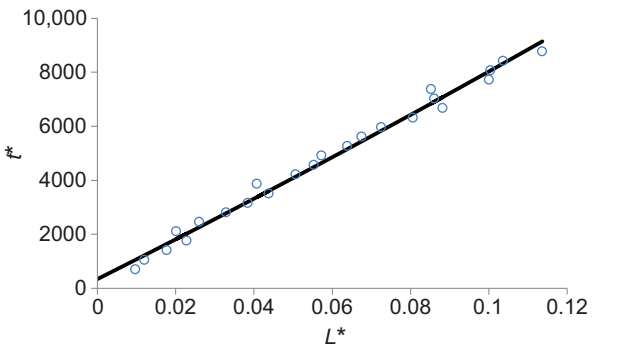


**Fig. 4. The dimensionless meniscus position ( $L^*$ ) versus dimensionless time ( $t^*$ ) for a single proboscis of the monarch butterfly.** Circles are experimental points and the solid line is the best fit with the proposed model.

proboscis, varied over a wide range, reflecting the different sizes of the tested proboscises (Table 1).

Suction-pump pressure

The following flow rates were obtained from the feeding experiments on droplets of aqueous sucrose solutions:  $\dot{Q}=0.5\times10^{-9}$  m<sup>3</sup> s<sup>-1</sup> ( $N=8$ , concentration=25%),  $\dot{Q}=0.3\times10^{-9}$  m<sup>3</sup> s<sup>-1</sup> ( $N=8$ , concentration=40%),  $\dot{Q}=0.2\times10^{-9}$  m<sup>3</sup> s<sup>-1</sup> ( $N=8$ , concentration=56%). We theoretically analyzed the pressure that would be needed in the butterfly's suction pump to support these flow rates in feeding experiments (Fig. 5). In these calculations, the viscosities of sucrose solutions were measured by magnetic rotational spectroscopy (Tokarev et al., 2013) and the densities of the sucrose solutions were taken from published values (Asadi, 2005) (Table 2).

The proboscis was modeled as a conduit consisting of a truncated cone and a straight tube of length  $L_p-H$ . We assumed that the point  $L_p$  corresponded to the position where the food canal meets the suction pump (i.e. the pressure at this point must be equal to the pressure in the suction pump). The basic Eqns A7 and A12 (see Appendix) were applied to determine the pressure at the conjunction point  $H$  and at the point  $L_p$ . The following materials parameters of the proboscis were used to calculate the pressure differentials at different regions:  $H=1.5$  mm,  $L_p=14$  mm,  $R_0=5$   $\mu$ m,  $R_p=30$   $\mu$ m and  $\tan\phi=0.0167$ . The pressure needed to pump fluid through a tapered proboscis was greater than possible at surface atmosphere, whereas the pressure needed in a straight tube was considerably less and within the realm of possibility (Fig. 5).

Feeding behavior

We observed that butterflies, while feeding, altered the configuration of the proboscis in four ways (Table 3, Fig. 6): (1) apically spreading the galeae ('galeal splaying'); (2) shifting the galeae along one

**Table 1. Dimensionless parameter ( $\beta$ ), radius of the terminal opening ( $R_0$ ) and length of the drinking region ( $H$ ) of the proboscis of the monarch butterfly**

Butterfly	$\beta (\times 10^4)$	$R_0 (\mu\text{m})$	$H (\text{mm})$
Monarch s1	1.5 $\pm$ 0.2	4.1 $\pm$ 0.2	1.55 $\pm$ 0.01
Monarch s2	8.0	3.2	1.60
Monarch s3	6.5 $\pm$ 0.7	3.5 $\pm$ 0.1	1.59 $\pm$ 0.01
Monarch s4	4.2 $\pm$ 1.8	4.1 $\pm$ 0.6	1.55 $\pm$ 0.04
Monarch s5	20.4 $\pm$ 4.7	2.4 $\pm$ 0.2	1.66 $\pm$ 0.01
Monarch s6	9.9 $\pm$ 6.4	2.9 $\pm$ 0.2	1.62 $\pm$ 0.01
Monarch s7	4.2 $\pm$ 2.4	4.2 $\pm$ 0.7	1.54 $\pm$ 0.04

Three measurements were obtained per butterfly, except for Monarch s2, for which there was one.

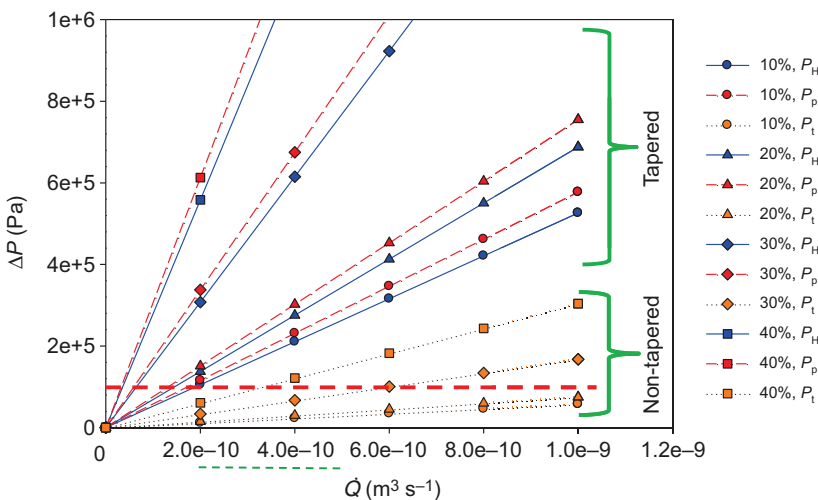


**Fig. 5. Pressure required to provide flow in tapered and non-tapered theoretical models of butterfly proboscises.**  $P_H$  is the pressure differential required in a tapered food canal at the drinking region (position  $H$  in Fig. 3);  $P_p$  is the pressure differential in the cibarial pump in a tapered food canal (position  $L_p$  in Fig. 3);  $P_t$  is the pressure differential in the cibarial pump in the drinking-straw (non-tapered) model when the radius ( $R_p$ ) of the food canal does not change along the proboscis. Percentages indicate aqueous sucrose concentrations. The red horizontal dashed line at 1 atm indicates the maximum limit of pressure differential that could be produced by the cibarial pump. The dashed line below the x-axis indicates the measured flow rates for monarch butterflies.

another in antiparallel movements (‘galeal sliding’); (3) radially expanding and contracting each galea (‘galeal pulsing’); and (4) forcing the proboscis against a surface (‘galeal pressing’). Each butterfly performed at least one of these behaviors while feeding on two to four droplets of 15% sucrose solution.

During galeal splaying, the two galeae separated slightly at their apices over a variable portion of the drinking region, whereas during galeal sliding, the galeae remained paired but moved along one another in antiparallel fashion for a distance of up to three proboscis diameters. During galeal sliding, one galea shifted toward the head, opening the end of the proboscis; the inner face of the food canal of the steady galea remained open for 0.1–90.0 s. Galeal pulsing involved rapid (0.05–0.30 s) expansion and contraction of each galea. Galeal sliding and pulsing were performed by individual butterflies independently or sequentially in the same feeding trial. Butterflies feeding on large drops pressed their proboscises to the substrate, alternately increasing and decreasing the proboscis diameter by as much as 5–8%.

DISCUSSION

In experiments on monarchs feeding from large droplets intended to simulate pools of liquid, the flow rates vary from  $0.2 \times 10^{-9}$  to  $0.5 \times 10^{-9} \text{ m}^3 \text{ s}^{-1}$ . Similar flow rates have been obtained for other species of butterflies (May, 1985). The sucrose solutions that we tested (25–56%) include sugar concentrations in flowers visited by Lepidoptera (Heinrich, 1975; Adler, 1987). These experiments set the metrics for the flow rates of interest. Using theoretical models of proboscises with tapered and smooth channels, we estimated the pressure required by a suction pump to support these, and greater, flow rates. Based on the model that a tapered tube more accurately approximates actual proboscis structure, we found that the pressure differential in the suction pump at the observed flow rates should be greater than 1 atm. Estimates for blood- and sap-feeding bugs support the need for high pressure differentials (Bennet-Clark, 1963;

Malone et al., 1999). Even for dilute sucrose solutions (e.g. 10%), the pressure differential is expected to be greater than 1 atm. However, no vacuum pump can produce a pressure differential greater than 1 atm in surface atmosphere (i.e. in an open system). Kingsolver and Daniel also point out that pressure differentials of more than 1 atm would be a mechanical limitation to butterfly feeding (Kingsolver and Daniel, 1979). In the drinking region where the food canal tapers, the pressure drops significantly, and the proximal portion of the proboscis makes a minor contribution to the pressure differential, as indicated (Fig. 5) by the close approximation of paired lines for pressure at the drinking region ( $P_H$ ) and in the cibarial pump ( $P_p$ ). Thus, more than 1 atm of pressure differential would need to be generated by the pump or another mechanism(s) to overcome the restriction of the tapered food canal in the drinking region; less force would be needed in the absence of a taper.

A tapered proboscis and food canal are characteristic of Lepidoptera (Krenn and Muhlberger, 2002); thus, the role of the taper in influencing the pressure differential is likely to be widespread among butterflies and moths. Moreover, a tapered food canal might be characteristic of most, if not all, fluid-feeding insects with an elongated proboscis, regardless of fluid source or type. Thus, insects such as blood-sucking true bugs and mosquitoes, sap-feeding planthoppers and nectar-feeding flies all have a tapered food canal (Christophers, 1960; Bennet-Clark, 1963; Malone et al., 1999; Karolyi et al., 2013). Butterflies, however, have a distinct feature; the proboscis has pores along its length that provide opportunities for air to enter or cavitation to occur. When butterflies use the cibarial pump to move liquid up the food canal, menisci in the interlegular slits deform to follow the pressure gradient. A similar effect can be observed by stretching a sponge completely filled with water; the water moves from the sides of the sponge, reflecting the change of pressure in the liquid column. When suction pressure is high, an air bubble can enter the food canal through the interlegular slits, supporting the partitioning of the liquid column. Also, to obtain feeding rates, we submersed the butterfly proboscis in fluid to avoid air in the food canal. However, under natural feeding conditions, air would enter the porous proboscis. Thus, the butterfly proboscis is not a closed system.

We recently showed that structural features of the drinking region, including tapering of the food canal, facilitate fluid acquisition by enhancing capillary action, allowing butterflies to drink from porous surfaces, such as damp soil (Monaenkova et al., 2012; Lehnert et al., 2013). Additional benefits of a tapered proboscis, with a concomitantly tapered food canal, include reduced costs associated

**Table 2. Properties of model nectars**

Sucrose concentration	$\eta$ (mPa s)	$\rho$ (kg m <sup>-3</sup> )
10%	1.3±0.2	1040
20%	1.7±0.2	1083
30%	3.8±0.4	1129
40%	6.9±0.7	1179

Data are from table A1 in Asadi (Asadi, 2005).  
 $\eta$ , liquid viscosity;  $\rho$ , liquid density.

**Table 3. Behavioral actions that might reduce the pressure differential in lepidopteran proboscises and enhance fluid uptake**

Activity	Evidence	Postulated effect	Cycle time	Other consequences
Galeal splaying	Tips separate	Opens food canal	<0.1 s	Cleans debris from tip of proboscis
Galeal sliding	Tips displace	Widens lumen beyond the taper	0.1–90.0 s	Allows air to enter and form bridges and menisci
Galeal pulsing	Galeal width changes by 5–8% of proboscis diameter	Increases lumen size and opens pores between legulae	0.05–0.30 s	Cleans legulae
Galeal pressing	Proboscis diameter increases and decreases	Spreads legulae and increases interlegular spacing	0.2–0.3 s	Increases contact area of proboscis and substrate
Cibarial pump (for time comparison)	X-ray imaging (Monaenkova et al., 2012)	Generates suction pressure for fluid uptake	0.45–0.70 s	Facilitates swallowing

with cuticular thickening (Bauder et al., 2013) and the ability to reach fluid sequestered in small recesses. The benefits of a tapered food canal, however, are countered by increased viscous friction (Batchelor, 2000) that hinders flow. However, the required pressure can be significantly reduced when the taper is ignored, as in previous models (e.g. Kingsolver and Daniel, 1979); in most cases the required pressure drops below atmospheric pressure for the same flow rate.

Optimizing uptake from liquid films and menisci, versus pools, therefore, is contradictory; a small lumen enhances capillarity (Monaenkova et al., 2012), whereas a large lumen enhances flow (Kingsolver and Daniel, 1995; Vogel, 2003). In other words, fluid uptake by the butterfly proboscis presents a paradox: a simple drinking-straw model that ignores structural features of the proboscis avoids the catastrophic pressure differential, whereas incorporating actual proboscis structure – the taper – into the model causes the required pressure to skyrocket.

We suggest that the mechanism of fluid uptake is more complex than a strict drinking-straw analogy and that the paradox can be resolved by a suite of behavioral strategies (Table 3). Galeal sliding could adjust the fluid–pressure differential by changing the size of the interlegular pores and terminal opening and by reducing the active, tapered length of the food canal. The ability to slide the galeae in antiparallel movements (Krenn, 1997) is well documented for moths that pierce animal and plant tissues (Büttiker et al., 1996); it also occurs in nectar-feeding Lepidoptera (Kwauk, 2012) and could serve to adjust the pressure differential. Galeal sliding might facilitate meniscus formation and transport if the amount of fluid is minute and a droplet is trapped in the food canal. Galeal sliding also could facilitate debris removal from the legular linkage. Galeal splaying opens the distal tip of the proboscis and should function to reduce the pressure differential by increasing the diameter in the tapered region. Although we observed this behavior in the monarchs in only two instances, we have observed it regularly in Gulf fritillaries, *Agraulis vanillae*. Galeal pulsing might be controlled by processes similar to those that drive coiling and uncoiling of the proboscis. Uncoiling, for example, is achieved by increased hemolymph pressure in each galea,

brought about by contractions of the maxillary stipital muscles, whereas coiling is achieved by contractions of intrinsic galeal muscles (Wannenmacher and Wasserthal, 2003). When hemolymph is forced from the head into the galeal lumen, it would be expected to travel in a rapid wave, supporting peristaltic pumping of fluid and increasing interlegular spacing and the diameter of the food canal. Galeal pressing would alter the food canal diameter, the legular spacing and perhaps also the surface contact area for capillarity.

We previously showed that the full cibarial pump cycle takes 0.45–0.70 s at 25°C (Monaenkova et al., 2012). Galeal sliding can be slower, lasting 0.1–90 s, and can, therefore, be independent of the pump; the proboscis would be able to remain open for multiple pump cycles. Galeal pulsing occurs faster than the rate of contraction and expansion of the suction pump and, therefore, might facilitate flow within the first half of the cycle when the pump is open. More experiments are required to test this hypothesis.

**MATERIALS AND METHODS**

**Preparation of proboscises**

Proboscises of unfed monarch butterflies (Shady Oak Butterfly Farm, Brookner, FL, USA) for scanning electron microscopy (Fig. 1) were straightened with crisscrossed pins on foam, dehydrated through an ethanol series (80–100%), dried in hexamethyldisilazane, mounted with double-sided conductive adhesive tape on aluminium stubs, and sputter coated with platinum for 3 min. Imaging was done with a Hitachi TM3000 (Hitachi High Technologies America Inc., Alpharetta, GA, USA) at 15 kV, composite image mode and full vacuum.

Coiled proboscises of seven monarch butterflies were soaked in deionized water for 12 h to soften and uncoil them; deionized water was used to maintain consistency across measurements and instruments. They were straightened several millimeters every 2 h and fixed in position with pins. Straightened proboscises were examined with an optical microscope to confirm that the galeae did not separate apically and to measure the diameter of the proboscis.

**Observations of feeding behavior**

To understand fluid uptake from pools of liquid, feeding behavior was observed under a stereomicroscope at 22±3°C. Monarch butterflies (*N*=5)

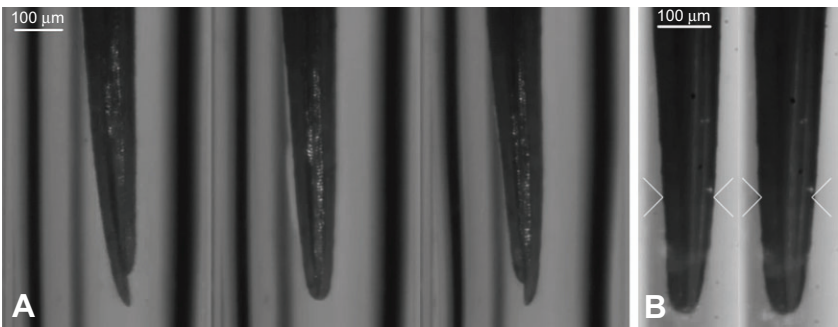


**Fig. 6. Image sequences extracted from a video recording of the proboscis tip of a monarch butterfly during feeding.** The proboscis must be flexible to contract and expand quickly when the butterfly feeds. (A) Galeal sliding. (B) Galeal pulsing; the arrowheads are plotted to show the incremental change of the proboscis size. In the left image the arrowheads point to the proboscis boundary, while in the right image the proboscis boundary expands, making the arrowheads indented into the proboscis. The degree of expansion varies along the proboscis.

were held by their wings, and their proboscises were threaded into glass capillary tubes (internal diameter=0.4 mm). A 15% sucrose solution was introduced into the opposite end of the capillary tube via flexible tubing. Butterflies were allowed to feed for 2–3 min and the behavior was video recorded (Dalsa Falcon 1.4M100 XDR). The drinking region of the proboscis was submersed in fluid throughout observations to maintain fluid in the food canal.

We also used an inverted microscope to observe feeding behavior of butterflies ( $N=5$ ) from droplets (1–2 ml each) of 15% sucrose solution placed on the microscope stage. Each butterfly was exposed to the droplets for 5–10 min. The drinking region of the proboscis remained submersed during feeding. Within a period of 5–10 min, each time a droplet was taken up by the butterfly, an additional droplet was added; each butterfly took up a total of two to four droplets.

To estimate uptake rate, butterflies were fed from large droplets (radius  $r_d=3$ –4 mm,  $h_d=2$ –3 mm) of sucrose solution (Fig. 7A). The droplets were modeled as hemispherical caps with volume  $V_d=(\pi h_d/6)(3r_d^2+h_d^2)$ . We therefore could minimize the effect of confinement and associated counter-pressure caused by viscous drag typically present (Cohn, 1954; Cohn, 1955; Rashevsky, 1960) when a butterfly is fed from a tube. Once the butterflies began drinking, they were not restrained at the stage. The feeding process was filmed with a high-speed camera (Motion ProX3, Redlake). The images were analyzed with ImageJ software (NIH), and the change in droplet volume was plotted as a function of time; the results were fitted with a straight line, with the slope indicating the uptake rate (Fig. 7B).

### Experiment design

The Cahn DCA-322 allowed incremental changes in the sample mass to be detected with 1  $\mu\text{g}$  accuracy. Each straightened proboscis was cut with a razor blade (single edge, Stanley) 5 mm proximal to its tip, and the cut end was inserted into a capillary tube. The inserted portion was ~3 mm long; the remaining (distal) 2 mm, which included the drinking region, protruded from the capillary tube. The tube with the proboscis was placed in a rectangular vessel (polystyrene, 12.5×12.5×45 mm, Plastibrand) and capped (Cuvette cap square, Fisher Scientific). A 3 mm diameter hole in the cap allowed the capillary tube to hang freely in the container, but permitted the Cahn balance arm to connect to it (Fig. 2A). The tip of the proboscis was suspended above the water, without touching it (Fig. 2B). A drop of motor oil (Castrol, SAE 5W-30) was used to seal the space between the hole edges and external wall of the tube, preventing evaporation and serving as a lubricant to enable the tube to move during wicking experiments. The tip of the proboscis was brought in contact with the water by raising the stage with the water vessel at  $20 \mu\text{m s}^{-1}$  (Fig. 2C). From the control experiments, we found that the trapped air bubble separating the top of the sealed vessel from the water surface required about 1 h to reach full saturation with water vapor (99% relative humidity, RH) when the water filled the vessel to a height of  $y=30$  mm.

### Data acquisition

Two loops were used for force measurements (loop a and loop b; Fig. 2A). Loop a could measure a force up to 1.5 mN; loop b was less sensitive and

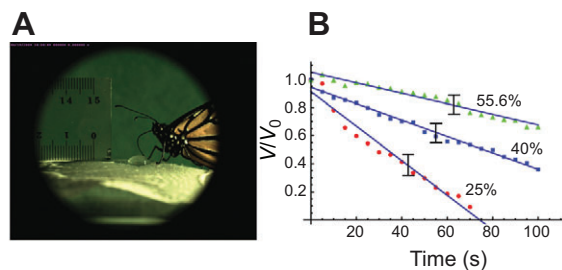


**Fig. 7. Determination of droplet volume and sucrose concentrations fed from by monarch butterflies.** (A) Monarch butterfly feeding from a droplet of sucrose as an example of an image used for estimation of droplet volume. (B) Dynamics of the change in droplet volume  $V$  with respect to initial volume  $V_0$  as a function of time for three sucrose concentrations; standard errors are from eight different experiments for each sucrose concentration.

could measure a force up to 7.5 mN. A reference weight on loop c was used to counterbalance the sample weight, allowing maximum sensitivity. The ratio of the applied masses on the three loops (a:b:c) was 1:5:1, meaning that a 100 mg sample on loop a or loop c created the same torque as a 500 mg sample on loop b.

A special function of the Cahn DCA-322 – the zero depth of immersion (ZDOI) – can set the starting moment for weight measurements. The moment when the proboscis tip first touched the water was chosen as the ZDOI point; we experimentally found that this point could be distinguished by setting a minimum force threshold of  $F_{\min}=5 \mu\text{N}$ . With this choice of the ZDOI point, if the measured force was less than  $5 \mu\text{N}$ , the stage continued upward movement. The balance was zeroed; when the stage moved up, the force became negative due to friction and wiggling of the capillary tube (Miller et al., 1983). However, this background noise was less than  $5 \mu\text{N}$ , and was not recorded (Fig. 8). When the proboscis touched the water, the force rapidly increased, reflecting the action of the wetting force, which was significantly larger than the ZDOI threshold (Miller et al., 1983). The friction on the capillary tube exerted by the lubricating layer of oil was always smaller than the threshold value  $F_{\min}$ .

When the tip of the proboscis touched the water and the measured force became greater than  $F_{\min}$ , the stage continued to rise up to 0.1 mm at  $20 \mu\text{m s}^{-1}$ , confirming that the proboscis tip was immersed in water. A negative slope in Fig. 8 was associated with the immersion process and was caused by buoyancy and increased viscous friction forces at the meniscus when the proboscis became immersed (Miller et al., 1983). The stage was then stopped. The entire setup was allowed 1 min to stabilize before acquiring the force change for the next 60 min (red line, Fig. 8). After the stage was stopped, a meniscus inside the capillary tube was observed, and all incremental changes of force detected by the analyzer were attributed to the incremental change of weight of the water column invading the tube as a result of capillary action.

### Measurement of surface tension ( $\sigma$ )

The surface tension of deionized water was measured using the Wilhelmy method with the Cahn DCA-322 (Adamson and Gast, 1997). A platinum wire (250  $\mu\text{m}$  diameter) was used as a standard probe (Miller et al., 1983). The wire was cleaned with ethanol and heated to red-hot with an oxidizing flame. The Wilhelmy equation  $F=\sigma p \cos\theta$  was used, where  $F$  is the wetting force and  $p$  is the perimeter of the probe. The contact angle was assumed to be zero,  $\theta=0$  deg; hence,  $\cos\theta=1$  because of the high surface energy of the platinum (Miller et al., 1983). Deionized water was measured three times, yielding an average surface tension of  $\sigma=71.4\pm0.5 \text{ mN m}^{-1}$ .

### Determining Jurin height ( $Z_c$ ) of a capillary tube

The contact angle of the internal meniscus was measured indirectly by analyzing the Jurin height ( $Z_c$ ), defined as the maximum possible height of the liquid column co-existing with the liquid reservoir (Jurin, 1917–1919):  $Z_c=P_c/pg=2\sigma\cos\theta/(pgr)$ . Deionized water ( $\eta$ : 1 mPa s,  $\rho$ : 1000  $\text{kg m}^{-3}$ ) in a

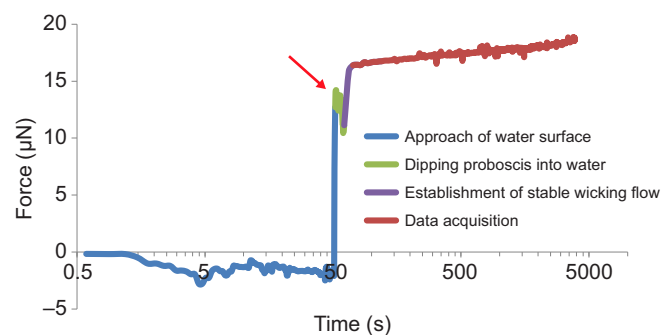


**Fig. 8. Typical experimental curve showing force changes at different steps of stage movement.** A steep jump of the blue line allowed the zero depth of immersion (ZDOI) point to be defined. The proboscis was immersed farther into the water for 0.1 mm (green line). After 1 min (purple line), the change of water weight for 60 min was collected (red line). Arrow indicates the ZDOI threshold.

glass capillary tube with a 250  $\mu\text{m}$  radius ( $r$ ) was used to determine the Jurin length at room temperature (20–21°C). Three experiments were performed, and the average Jurin height was calculated as  $Z_c = 0.029 \pm 0.001$  m.

## APPENDIX

### Derivation of the basic equations to determine permeability of the butterfly proboscis

The center of Cartesian coordinates was taken at the water surface, with the  $y$ -axis pointing upward. The flow potential  $\Phi$  was introduced as the sum of the pressure in water  $P(y)$  at position  $y$  and hydrostatic pressure due to the weight of the liquid column:

$$\Phi = P(y) + \rho g y, \quad (\text{A1})$$

where  $\rho$  is water density and  $g$  is acceleration due to gravity. By this definition, the pressure at the water surface is zero and the potential is zero. Thus, Darcy's law is written through the flow potential as  $\dot{Q} = -k_p A / \eta (\partial \Phi / \partial y)$ , where  $k_p$  is the permeability of the proboscis,  $\eta$  is the liquid viscosity and  $\partial \Phi / \partial y$  is the potential gradient along the proboscis. With this definition of permeability, the material parameter  $k_p$  could be obtained by measuring the total flow rate ( $\dot{Q}$ ) and the potential gradient and by knowing the proboscis cross-sectional area and viscosity of liquid used in our experiments. We measured the flow rate directly with a Cahn DCA-322, but the potential gradient was not defined. Therefore, data interpretation required additional information regarding fluid flow. Below, a model is presented to allow us to extract the permeability from the experimental data.

### Liquid discharge through the drinking region of the food canal ( $\dot{Q}_H$ )

The cross-sectional area in the drinking region of the food canal,  $A$ , changes from the tip to the proximal end of the drinking region. The shape of the food canal in the drinking region was assumed to be conical (Fig. 7). The radius of the food canal at the submerged tip is denoted by  $R_0$ , and the radius of the food canal at the proximal end of the drinking region is denoted by  $R_p$ . Introducing the cone angle  $\varphi$ , the radius of the food canal at position  $y$  from the tip is expressed as  $R(y) = R_0 + y \tan \varphi$ . Using the Hagen–Poiseuille law and assuming that the taper angle is small, we approximated the permeability of the drinking region of the food canal as  $k_H = (R_0 + y \tan \varphi)^2 / 8$ . Accordingly, water discharge through a cross-sectional area  $A(y)$  is expressed as:

$$\dot{Q}_H = -\frac{k_H A(y)}{\eta} \frac{\partial \Phi_H}{\partial y} = -\frac{\pi (R_0 + y \tan \varphi)^4}{8\eta} \frac{\partial \Phi_H}{\partial y}, \quad (\text{A2})$$

where subscript H refers to the drinking region. The flow discharge through any proboscis cross-section  $y$  is the same at any time moment  $t$ ,  $\dot{Q}_H = \dot{Q}_H(t)$ . Substituting this relationship into Eqn A2 and integrating it, we get:

$$\int_0^H \frac{8\eta \dot{Q}_H(t) dy}{\pi (R_0 + y \tan \varphi)^4} = -\Phi_H(H) = -(P_H + \rho g H), \quad (\text{A3})$$

where  $H$  is the drinking region length and  $P_H$  is the pressure at the end of the food canal. Solving Eqn A3 for  $\dot{Q}_H$ , the liquid discharge through the drinking region of the food canal is expressed as:

$$\dot{Q}_H(t) = -(P_H + \rho g H) \int_0^H \frac{8\eta dy}{\pi (R_0 + y \tan \varphi)^4}. \quad (\text{A4})$$

### Liquid discharge through the non-drinking region of the food canal ( $\dot{Q}_p$ )

Proximal to the drinking region,  $y > H$ , the cone angle  $\varphi$  of the food canal becomes small (Fig. 3) and the food canal in the non-drinking

region is modeled by a straight cylindrical tube with radius  $R_p$ . Therefore, the flow of the liquid column can be described by the Hagen–Poiseuille law (Adamson and Gast, 1997) written in Darcy's form as  $\dot{Q}_p = -(k_p A / \eta) (\partial \Phi_p / \partial y)$ , with  $k_p = R_p^2 / 8$ . Subscript p refers to the non-drinking region of the food canal. Using the mass conservation equation, we obtain  $\partial \dot{Q}_p / \partial y = \partial^2 \Phi_p / \partial y^2 = 0$ . By integrating this equation, the linear distribution of the potential along the liquid column,  $\Phi_p = cy + d$ , can be inferred, where  $c$  and  $d$  are time-dependent functions that can be found from the boundary conditions. The boundary conditions state that the pressure at the end of the drinking region of the food canal,  $y = H$ , must be equal to the pressure in the water column at the same position,  $y = H$ . Therefore,  $P_H + \rho g H = cH + d$ . At the inserted end of the food canal,  $y = L_p$ , the pressure is written as  $P_p + \rho g L_p = cL_p + d$ . From these two boundary conditions, it follows that  $c = [P_p - P_H + \rho g (L_p - H)] / (L_p - H)$  and  $d = P_p + \rho g L_p - L_p [P_p - P_H + \rho g (L_p - H)] / (L_p - H) = P_H + H(P_p - P_H) / (L_p - H)$ . With the obtained constants, liquid discharge through the rest of the food canal is expressed as:

$$\dot{Q}_p = -(k_p A / \eta) a = -\frac{\pi R_p^4}{8\eta} [P_p - P_H + \rho g (L_p - H)] / (L_p - H). \quad (\text{A5})$$

The pressure at the end of the drinking region of the food canal,  $P_H$ , can be related using the conservation of mass,  $\dot{Q}_H = \dot{Q}_p$ :

$$-(P_H + \rho g H) \int_0^H \frac{8\eta dy}{\pi (R_0 + y \tan \varphi)^4} = -\frac{\pi R_p^4}{8\eta} [P_p - P_H + \rho g (L_p - H)] / (L_p - H). \quad (\text{A6})$$

Taking the integral and using the definition  $R_p = R_0 + H \tan \varphi$ , we can express the pressure  $P_H$  as:

$$P_H = \frac{b P_p + \rho g b (L_p - H) - \rho g a H}{a + b}, \quad (\text{A7})$$

where we introduce the constants:

$$a = 3 \tan \varphi R_0^3 R_p^3 / (R_p^3 - R_0^3) \quad (\text{A8})$$

and

$$b = R_p^4 / (L_p - H). \quad (\text{A9})$$

These constants contain the structural parameters of the proboscis. Plugging Eqn A7 into Eqn A4, the liquid discharge through the non-drinking region of the food canal is expressed as:

$$\dot{Q}_p = -\frac{\pi a b}{8\eta(a + b)} (P_p + \rho g L_p). \quad (\text{A10})$$

### Meniscus motion through the capillary tube and related water discharge ( $\dot{Q}_c$ )

Liquid discharge through the capillary tube is the same as that given by Eqn A4. Conservation of mass requires the equality  $\dot{Q}_p = \dot{Q}_c$ , where the flow rate through the capillary tube is given by the Hagen–Poiseuille law, with the pressure at one end  $y = L_p$  being  $P_p$  and at the other end, that is, at the meniscus position  $y = L_p + L(t)$ , being  $P_c$ :

$$-\frac{\pi a b}{8\eta(a + b)} (P_p + \rho g L_p) = -\frac{\pi r^4}{8\eta} [P_p + P_c + \rho g (L_p - L)] / (L_p - L). \quad (\text{A11})$$

Solving this equation for  $P_p$  yields:

$$P_p = \frac{1}{\left(\frac{ab}{a+b} - \frac{r^4}{L_p - L}\right)} \left[ \frac{r^4 P_c}{L_p - L} + \frac{\rho g r^4}{L_p - L} (L_p - L) - \frac{\rho g a b L_p}{a+b} \right]. \quad (\text{A12})$$

Plugging Eqn A12 into Eqn A7 and then into Eqn A4 and expressing its left side through the meniscus velocity  $\dot{Q}_c = \pi r^2 dL/dt$ , the basic equation describing the kinetics of meniscus propagation through the complex conduit consisting of the proboscis and capillary tube is expressed as:

$$\frac{dL}{dt} = \frac{r^2}{8\eta} \frac{(P_c - \rho g L)}{L - L_p + \frac{r^4(a+b)}{ab}}. \quad (\text{A13})$$

#### Acknowledgements

We thank Bethany Kauffman, Steven Rea, and Taras Andrukh for helping with high-speed imaging of butterfly feeding behavior.

#### Competing interests

The authors declare no competing financial interests.

#### Author contributions

C.-C.T. prepared the samples, designed and performed all permeability experiments, and analyzed data; D.M. performed all feeding experiments with live butterflies and analyzed data; C.E.B. prepared samples and conducted SEM imaging; P.H.A. conceived the project, prepared samples, and analyzed data; K.G.K. conceived the project, designed experiments, set up the models, analyzed data and, together with P.H.A. and C.E.B., wrote the manuscript.

#### Funding

This work was supported by the National Science Foundation through Grants EFRI 0937985 and PoLS 1305338.

#### References

- Adamson, A. W. and Gast, A. P. (1997). *Physical Chemistry of Surfaces*. New York, NY: Wiley.
- Adler, P. H. (1987). Temporal feeding patterns of adult *Heliothis zea* (Lepidoptera: Noctuidae) on pigeonpea nectar. *Environ. Entomol.* **16**, 424-427.
- Asadi, M. (2005). *Beet-Sugar Handbook*, pp. 779-801. Hoboken, NJ: John Wiley & Sons, Inc.
- Barth, F. G. (1991). *Insects and Flowers: The Biology of a Partnership*. Princeton, NJ: Princeton University Press.
- Batchelor, G. K. (2000). *An Introduction to Fluid Dynamics*. New York, NY: Cambridge University Press.
- Bauder, J. A.-S., Handschuh, S., Metscher, B. D. and Krenn, H. W. (2013). Functional morphology of the feeding apparatus and evolution of proboscis length in metalmark butterflies (Lepidoptera: Riodinidae). *Biol. J. Linn. Soc. Lond.* **110**, 291-304.
- Bennet-Clark, H. C. (1963). Negative pressures produced in the pharyngeal pump of the blood-sucking bug, *Rhodnius prolixus*. *J. Exp. Biol.* **40**, 223-229.
- Borrell, B. J. (2006). Mechanics of nectar feeding in the orchid bee *Euglossa imperialis*: pressure, viscosity and flow. *J. Exp. Biol.* **209**, 4901-4907.
- Borrell, B. J. and Krenn, H. W. (2006). Nectar feeding in long-proboscid insects. In *Ecology and Biomechanics: A Mechanical Approach to the Ecology of Animals and Plants* (ed. A. Herrel, T. Speck and N. P. Rowe), pp. 185-205. Boca Raton, FL: CRC.
- Büttiker, W., Krenn, H. W. and Putterill, J. F. (1996). The proboscis of eye-frequenting and piercing Lepidoptera (Insecta). *Zoomorphology* **116**, 77-83.
- Christophers, S. R. (1960). *Aedes aegypti* (L.) the Yellow Fever Mosquito: Its Life History, Bionomics and Structure. London: Cambridge University Press.
- Cohn, D. L. (1954). Optimal systems: I. The vascular system. *Cohn. Bull. Math. Biophys.* **16**, 59-74.
- Cohn, D. L. (1955). Optimal systems: II. The vascular system. *Bull. Math. Biophys.* **17**, 219-227.
- Dullien, F. A. L. (1991). *Porous Media: Fluid Transport and Pore Structure*. New York, NY: Academic Press.
- Eastham, L. E. S. and Eassa, Y. E. E. (1955). The feeding mechanism of the butterfly *Pieris brassicae* L. *Philos. Trans. R. Soc. B* **239**, 1-43.
- Grimaldi, D. and Engel, M. S. (2005). *Evolution of the Insects*. New York, NY: Cambridge University Press.
- Heinrich, B. (1975). Energetics of pollination. *Annu. Rev. Ecol. Syst.* **6**, 139-170.
- Jurin, J. (1917-1919). An account of some experiments shown before the Royal Society; with an enquiry into the cause of the ascent and suspension of water in capillary tubes. *Philos. Trans. R. Soc.* **30**, 1717-1719.
- Karolyi, F., Morawetz, L., Colville, J. F., Handschuh, S., Metscher, B. D. and Krenn, H. W. (2013). Time management and nectar flow: flower handling and suction feeding in long-proboscid flies (Nemestrinidae: Prosoeca). *Naturwissenschaften* **100**, 1083-1093.
- Kingsolver, J. G. (1985). Butterfly engineering. *Sci. Am.* **253**, 106-113.
- Kingsolver, J. G. and Daniel, T. L. (1979). On the mechanics and energetics of nectar feeding in butterflies. *J. Theor. Biol.* **76**, 167-179.
- Kingsolver, J. G. and Daniel, T. L. (1995). Mechanics of food handling by fluid-feeding insects. In *Regulatory Mechanisms in Insect Feeding* (ed. R. F. Chapman and G. de Boer), pp. 32-74. New York, NY: Springer.
- Knopp, M. C. N. and Krenn, H. W. (2003). Efficiency of fruit juice feeding in *Morpho peleides* (Nymphalidae, Lepidoptera). *J. Insect Behav.* **16**, 67-77.
- Krenn, H. W. (1997). Proboscis assembly in butterflies (Lepidoptera) – a once in a lifetime sequence of events. *Eur. J. Entomol.* **94**, 495-501.
- Krenn, H. W. (2010). Feeding mechanisms of adult Lepidoptera: structure, function, and evolution of the mouthparts. *Annu. Rev. Entomol.* **55**, 307-327.
- Krenn, H. W. and Kristensen, N. P. (2000). Early evolution of the proboscis of Lepidoptera: external morphology of the galea in basal glossatan moths, with remarks on the origin of the pilifers. *Zool. Anz.* **239**, 179-196.
- Krenn, H. W. and Muhlberger, N. (2002). Groundplan anatomy of the proboscis of butterflies (Papilionoidea, Lepidoptera). *Zool. Anz.* **241**, 369-380.
- Kristensen, N. P. (1984). Studies on the morphology and systematics of primitive Lepidoptera (Insecta). In *Steenstrupia*, Vol. 10, No. 5, pp. 141-191. Copenhagen: Copenhagen Zoological Museum.
- Kwauk, K. J. (2012). Fluid uptake by the lepidopteran proboscis in relation to structure, Clemson, SC: Clemson University.
- Lehane, M. J. (2005). *The Biology of Blood-Sucking in Insects*. New York, NY: Cambridge University Press.
- Lehnert, M. S., Monaenkova, D., Andrukh, T., Beard, C. E., Adler, P. H. and Kornev, K. G. (2013). Hydrophobic-hydrophilic dichotomy of the butterfly proboscis. *J. R. Soc. Interface* **10**, 20130336.
- Lucas, R. (1918). Ueber das zeitgesetz des kapillaren aufstiegs von flüssigkeiten. *Kolloid-Zeitschrift* **23**, 15-22.
- Malone, M., Watson, R. and Pritchard, J. (1999). The spittlebug *Philaenus spumarius* feeds from mature xylem at the full hydraulic tension of the transpiration stream. *New Phytol.* **143**, 261-271.
- May, P. G. (1985). Nectar uptake rates and optimal nectar concentrations of two butterfly species. *Oecologia* **66**, 381-386.
- Miller, B., Penn, L. S. and Hedvat, S. (1983). Wetting force measurements on single fibers. *Colloids and Surfaces* **6**, 49-61.
- Monaenkova, D., Lehnert, M. S., Andrukh, T., Beard, C. E., Rubin, B., Tokarev, A., Lee, W. K., Adler, P. H. and Kornev, K. G. (2012). Butterfly proboscis: combining a drinking straw with a nanosponge facilitated diversification of feeding habits. *J. R. Soc. Interface* **9**, 720-726.
- Rashevsky, N. (1960). *Mathematical Biophysics*. New York, NY: Dover Publications.
- Scheidegger, A. E. (1974). *The Physics of Flow Through Porous Media*. Toronto, ON: University of Toronto.
- Tokarev, A., Kaufman, B., Gu, Y., Andrukh, T., Adler, P. H. and Kornev, K. G. (2013). Probing viscosity of nanoliter droplets of butterfly saliva by magnetic rotational spectroscopy. *Appl. Phys. Lett.* **102**.
- Tsai, C.-C. and Kornev, K. G. (2013). Characterization of permeability of electrospun yarns. *Langmuir* **29**, 10596-10602.
- Tsai, C. C., Mikes, P., Andrukh, T., White, E., Monaenkova, D., Burtovyy, O., Burtovyy, R., Rubin, B., Lukas, D., Luzinov, I. et al. (2011). Nanoporous artificial proboscis for probing minute amount of liquids. *Nanoscale* **3**, 4685-4695.
- Vogel, S. (2003). *Comparative Biomechanics: Life's Physical World*. Princeton, NJ: Princeton University Press.
- Wannenmacher, G. and Wasserthal, L. T. (2003). Contribution of the maxillary muscles to proboscis movement in hawkmoths (Lepidoptera: Sphingidae) – an electrophysiological study. *J. Insect Physiol.* **49**, 765-776.
- Washburn, E. (1921). The dynamics of capillary flow. *Phys. Rev.* **17**, 273-283.